



Periodic waves in the lower thermosphere observed by OI630 nm airglow images

I. Paulino¹, A. F. Medeiros¹, S. L. Vadas², C. M. Wrasse³, H. Takahashi³, R. A. Buriti¹, D. Leite¹, S. Filgueira¹, J. V. Bageston³, J. H. A. Sobral³, and D. Gobbi³

¹Unidade Acadêmica de Física, Universidade Federal de Campina Grande, Campina Grande/PB, Brazil

²Colorado Research Associates, Northwest Research Associates, Boulder, CO 80301, USA

³Divisão de Aeronomia, Instituto Nacional de Pesquisas Espaciais, São José dos Campos/SP, Brazil

Correspondence to: I. Paulino (igopaulino@gmail.com)

Received: 6 August 2015 – Revised: 4 February 2016 – Accepted: 9 February 2016 – Published: 24 February 2016

Abstract. Periodic wave structures in the thermosphere have been observed at São João do Cariri (geographic coordinates: 36.5° W, 7.4° S; geomagnetic coordinates based on IGRF model to 2015: 35.8° E, 0.48° N) from September 2000 to November 2010 using OI630.0 nm airglow images. During this period, which corresponds to almost one solar cycle, characteristics of 98 waves were studied. Similarities between the characteristics of these events and observations at other places around the world were noted, primarily the spectral parameters. The observed periods were mostly found between 10 and 35 min; horizontal wavelengths ranged from 100 to 200 km, and phase speed from 30 to 180 m s⁻¹. These parameters indicated that some of the waves, presented here, are slightly faster than those observed previously at low and middle latitudes (Indonesia, Carib and Japan), indicating that the characteristics of these waves may change at different places. Most of observed waves have appeared during magnetically quiet nights, and the occurrence of those waves followed the solar activity. Another important characteristic is the quasi-monochromatic periodicity that distinguish them from the single-front medium-scale traveling ionospheric disturbances (MSTIDs) that have been observed previously over the Brazilian region. Moreover, most of the observed waves did not present a phase front parallel to the northeast–southwest direction, which is predicted by the Perkins instability process. It strongly suggests that most of these waves must have had different generation mechanisms from the Perkins instability, which have been pointed out as being a very important mechanism for the generation of MSTIDs in the lower thermosphere.

Keywords. Ionosphere (wave propagation) – meteorology and atmospheric dynamics (thermospheric dynamics; waves and tides)

1 Introduction

Atmospheric gravity waves (AGWs) have an important role in the dynamics of the Earth's atmosphere. They can transfer energy and momentum from the lower to the middle and upper atmosphere. When gravity waves propagate upward, they can interact with the background atmosphere, producing several effects for the dynamics and structure of the atmosphere. For instance, gravity waves can drive the quasi-biennial oscillation (QBO) in the stratosphere and can interact with planetary and tidal waves in the middle atmosphere. The impact of the turbulence arising from gravity waves is another important aspect to be considered. More details about the effects of gravity waves on the dynamics of the atmosphere are discussed in Fritts and Alexander (2003).

When wave structures are observed in the ionospheric parameters, they are called traveling ionospheric disturbances (TIDs). Depending on the size of the TID, they can be called small scale (SSTID), medium scale (MSTID) or large scale (LSTID). When medium-scale TIDs have periodic form, their wavelengths range from a few kilometers to several hundred kilometers. The associated periods range from a few minutes to a few hours (e.g., Hocke and Schlegel, 1996; Garcia et al., 2000). MSTIDs appear as a single traveling structure as well (e.g., Candido et al., 2008; Pimenta et al., 2008; Amorim et al., 2011).

MSTIDs have been observed from different techniques, like GNSS receivers (e.g., Saito et al., 1998; Otsuka et al., 2008; Kotake et al., 2006; Kutiev et al., 2009; Katamzi et al., 2012; Deng et al., 2013), airglow imaging (e.g., Mendillo et al., 1997; Taylor et al., 1998; Kubota et al., 2000; Sobral et al., 2001; Shiokawa et al., 2003, 2005, 2006, 2013; Otsuka et al., 2004, 2007; Martinis et al., 2011; Amorim et al., 2011; Fukushima et al., 2012; Smith et al., 2013; Narayanan et al., 2014), radio waves and onboard satellite observations (e.g., Waldock and Jones, 1987; He and Ping, 2008; Park et al., 2010; Vadas and Nicolls, 2009; Vadas and Crowley, 2010; MacDougall and Jayachandran, 2011; Frissell et al., 2014). Theoretical studies and reviews on MSTIDs have also been published elsewhere (e.g., Francis, 1974; Hocke and Schlegel, 1996; Fritts and Alexander, 2003; Yokoyama et al., 2008; Yokoyama and Hysell, 2010; Kelley, 2011).

One of the most important mechanisms that has been pointed out as being effective for generation of MSTIDs is the Perkins instability (Perkins, 1973). This mechanism occurs at middle latitudes in both hemispheres and can create waves in the ionosphere. Those waves have a phase front parallel to the northeast–southwest direction in the Southern Hemisphere and to the northwest–southeast direction in the Northern Hemisphere. They typically propagate toward the equatorial region, that is, toward the northwest in the Southern Hemisphere and toward the southwest in the Northern Hemisphere, but it depends on the direction of the thermospheric wind direction. Simulations made by Yokoyama et al. (2009) suggest that sporadic E layer instability plays a major role for the structures in the F region, which can propagate in that direction.

On the other hand, gravity waves are generated at all latitudes, can propagate in any direction, and are created in both the lower atmosphere (troposphere, stratosphere, mesosphere) and thermosphere. Through the effect of ion drag, those neutral oscillations push and pull the ions mainly along the magnetic field lines with the same period, thereby creating periodic waves in the ionosphere (Hocke and Schlegel, 1996; Nicolls et al., 2014). In contrast to the waves created by the Perkins instability, however, the phase front of gravity waves can have any direction (e.g., Fritts and Alexander, 2003). Typical lower-atmospheric gravity wave sources are deep convection (e.g., Vadas et al., 2009), wind flow over mountains (e.g., Smith et al., 2013), wind shear (e.g., Clemesha and Batista, 2008), etc. Thermospheric sources include body forcing and heating caused by the dissipation of gravity waves from the lower atmosphere (e.g., Vadas and Liu, 2009; Vadas, 2013) and increase of energy input into the system during the periods of enhanced geomagnetic activity (such as the aurora, for instance; Afraimovich et al., 2000; Ishida et al., 2008).

Airglow imaging is an useful tool with which to study the dynamics of the atmosphere. For instance, atmospheric gravity waves with different scales can be studied in the mesosphere and lower thermosphere (MLT), including the alti-

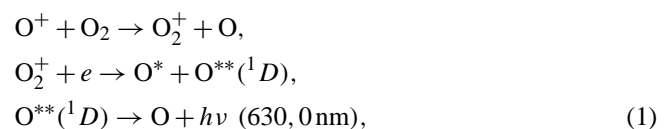
tudes of the ionospheric F region (e.g., Taylor et al., 1995, 1998, 2009). Periodic structures has been observed by airglow measurements of the thermospheric OI630 nm emission (e.g., Shiokawa et al., 2006; Taylor et al., 1998; Makela et al., 2011; Fukushima et al., 2012; Smith et al., 2013), but there is no consensus about where those waves have been generated. They could come from the lower levels of the atmosphere, or perhaps they are generated locally.

The purpose of the present work is to investigate the characteristics of periodic waves observed in the OI6300 airglow all-sky images over the Brazilian equatorial region. Using almost one solar cycle of data, 98 periodic waves were identified and their parameters (horizontal wavelength, period, phase speed and propagation direction) were estimated and studied. Wave structures like single-front were not included in the analysis. Since the present study is based on long-term measurements, the presence of seasonality and influences of the solar and magnetic activities on the occurrence of these waves were investigated as well.

2 Instrumentation and observation

An all-sky imager operated at São João do Cariri (geographic coordinates: 36.5° W, 7.4° S; geomagnetic coordinates based on IGRF model to 2015: 35.8° E, 0.48° N) from September 2000 to November 2010, which corresponds to almost one entire solar cycle. Airglow images of OH, O₂, OI557.7 nm (OI5577), OI630.0 nm (OI6300), and OI774.4 nm (OI7774) emissions were taken by this equipment, but in the present work only the OI6300 measurements were used. A total of 1013 cloudless nights were investigated during this period, which corresponds to over 7584 h of observation. Due to either maintenance or specific campaign mode operation, OI6300 images were not obtained in March and November 2001, October and November 2002, January 2004, February 2005, December 2005 through July 2006, May 2007, and April 2008.

The OI6300 airglow emission or red line of the atomic oxygen is produced on the bottom side of the ionospheric F region at around 220–280 km height. The emission mechanism is known to be a dissociative recombination, which chemically is expressed by



in which the photon emitted is in the red wavelength range.

This optical method, then, (of observing periodic waves via measurements of the OI6300 airglow intensity) is a good technique to investigate the propagation characteristics of gravity waves. High-frequency gravity waves with large vertical wavelengths (λ_z) can propagate to the ionospheric F layer (Vadas, 2007). There, they create perturbations in the

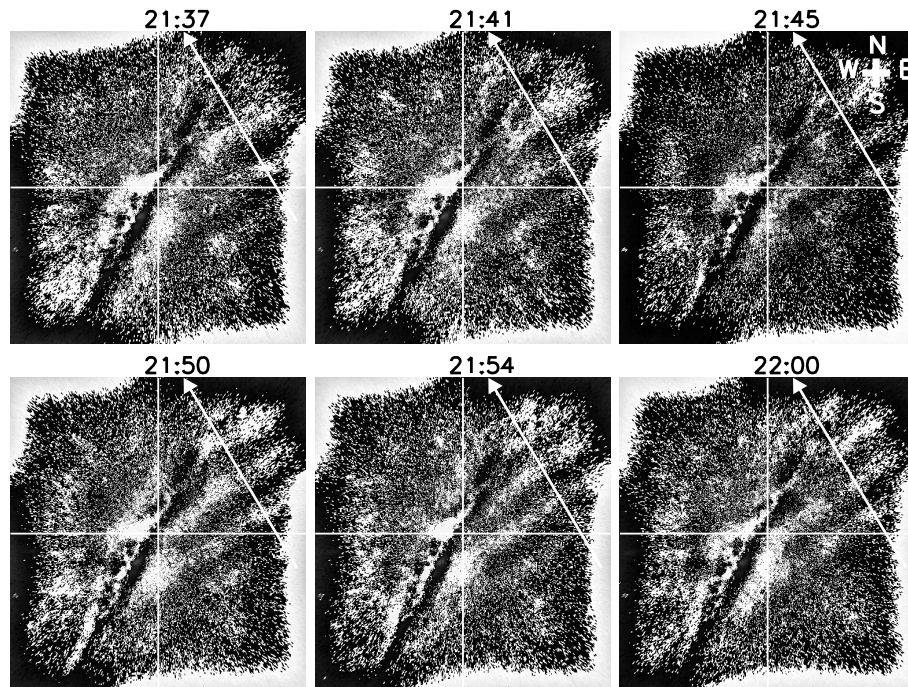


Figure 1. Sequence of unwarped images showing a gravity wave propagating to the northwest (north is to the top and east is to the right) observed on 20 September 2006. Universal time is shown at the top of the images. Darkened grooves in the center of the images represent the Milky Way. White arrows are pointed in the propagation direction of the wave. (See the movie in the Supplement for further details about the propagation of this periodic wave and the filtering process, <http://dx.doi.org/10.5446/17780>.)

neutral molecules that reside at that altitude. Ion drag then creates perturbations in the ions, which in turn creates perturbations in the electrons. This ultimately creates perturbations in the OI6300 airglow emission, as long as λ_z is much larger than $1/2$ times the thickness of the airglow emission layer; this requirement is necessary in order that the wave-induced perturbations do not average out for a viewer observing at the ground.

Since the OI6300 airglow layer is ~ 80 km thick (Sobral et al., 1993), the requirement for the OI6300 airglow layer is that $\lambda_z \gg 40$ km in order to observe a gravity wave in this emission layer. Comparing with Vadas (2007), this requirement is satisfied for medium-scale gravity waves having reasonably large intrinsic phase speeds of $c_H > 100 \text{ m s}^{-1}$. However, using only OI6300 airglow images, it is not possible to distinguish whether those periodic waves are gravity waves, generated in the neutral atmosphere, or are induced waves due to local ionospheric instability processes, like Perkins' waves.

From 10 years of observations, over 150 wave structures were detected in the OI6300 images. However, there were only 98 events among them for which we could effectively estimate their parameters by using two-dimensional Fourier analysis. As far as we know, this study presents the most extensive data on periodic waves observed in the OI6300 emission layer in the equatorial region.

The São João do Cariri airglow all-sky imager is an optical instrument composed of a fast ($f/4$) fish-eye and telecentric lens system, a filter wheel, a charged coupled device (CCD) camera, and a set of lens to reconstruct the images on the CCD. The whole system is controlled by a microcomputer. The CCD camera has a large area of 6.45 cm^2 , high resolution and a 1024×1024 back-illuminated CCD array with 14 bits per pixel. In order to enhance the signal-to-noise ratio, the images were binned on-chip down to a resolution of 512×512 . The high quantum efficiency, low dark noise (0.5 electrons/pixel/s), low readout noise (15 electron rms) and high linearity (0.05 %) of this device enable it to measure airglow emission. More details about the São João do Cariri imager have been reported by Medeiros et al. (2005).

Images of the OI6300 emission were taken by using an interference filter of 2 nm bandwidth and 3 in. diameter with an integration time of 90 s. The sampling rate of the OI6300 images was about once every 4 min. Since the airglow emissions are tenuous, observation were made during nighttime around the new-moon periods, which correspond to ~ 13 nights of observation per month.

Figure 1 shows an example of a periodic wave observed on 20 September 2006. The sequence of images in Fig. 1 was corrected to geographic coordinates and has a size of $1024 \text{ km} \times 1024 \text{ km}$. A Butterworth high-pass digital filter was applied to present images in order to emphasize the propagating form and direction, from southeast to northwest of

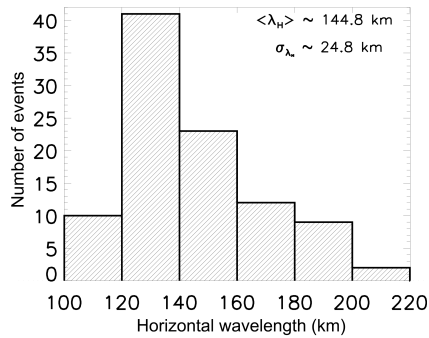


Figure 2. Histogram for the horizontal wavelength.

this periodic wave (see the movie in the Supplement for further details about the propagation of this periodic wave and the filtering process, <http://dx.doi.org/10.5446/17780>).

In order to estimate the horizontal parameters of the observed periodic waves, a spectral analysis was performed. The first step was to convert the images into the geographical coordinate system using the positions of stars in the image as reference points. It was assumed that the emission is from a layer centered around 240 km altitude. The horizontal wavelengths of the waves were estimated by applying a standard two-dimensional fast Fourier transform (FFT). In addition, to determine the period (and hence phase speed), the temporal one-dimensional FFT of the two-dimensional FFT in space was taken (e.g., Medeiros et al., 2003).

3 Results and discussion

3.1 Observed parameters

Using the technique described above, the parameters of 98 periodic waves were estimated. Figure 2 shows a statistical histogram of the observed horizontal wavelengths. Most of the waves had horizontal wavelengths (λ_H) between 120 and 160 km. The mean observed horizontal wavelength was 144.8 km with a standard deviation of 24.8 km. It is important to note that no wave had wavelengths either greater than 220 km or less than 60 km. Note that, using this technique, it is possible to observe periodic waves with horizontal wavelengths as long as 1500 km in the OI6300 images, which is the size of the projected area. Otherwise, theoretically gravity waves with wavelengths as short as the spatial resolution could be observed, but the shortest one had horizontal wavelength of ~ 67 km.

Figure 3 shows the observed periods (τ) for the quasi-monochromatic periodic waves. Most of them ranged from 10 to 35 min, indicating that they had short periods as compared to the medium-scale gravity waves observed in the MLT region (Taylor et al., 2009; Paulino et al., 2011). The mean period of these waves was 21.8 min with a standard deviation of 10.6 min. No wave had a period shorter than

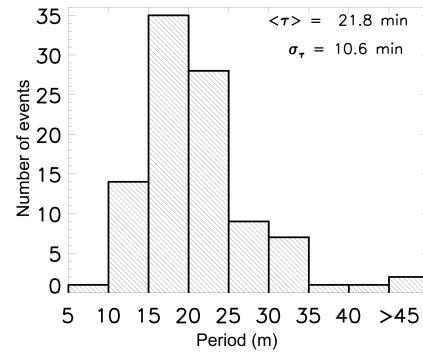


Figure 3. Histogram for the observed period.

5 min, and only two of them had periods larger than 45 min. The lower limit makes sense, given that gravity waves cannot have intrinsic periods shorter than the Brünt–Väissälä or buoyancy period, which is ~ 8 – 9 min at that altitude (Vadas, 2007).

Using the periods (τ) and horizontal wavelengths (λ_H) from Figs. 2 and 3, the observed horizontal phase speeds ($c_H = \lambda_H/\tau$) were estimated, and the results are shown in Fig. 4. Most of the waves had phase speeds between 60 and 150 m s^{-1} , although fewer had much larger phase speeds (up to 210 m s^{-1}). The mean phase speed was 109.0 m s^{-1} with a standard deviation of 37.5 m s^{-1} . Note that the phase speed is different from the intrinsic phase speed, from which the background wind has been subtracted (e.g., Fritts and Alexander, 2003).

Comparing the wave parameters estimated in this work to the results from Garcia et al. (2000), one can note that the wavelengths and periods were shorter than those from Arecibo, and the periodic waves observed over São João do Cariri are faster.

The present results indicate that the periodic waves observed in the OI6300 airglow emission were faster than the waves observed in the OH layer in the MLT region over Brazil from 2000 to 2004 (Medeiros et al., 2007) and during the Southern Hemisphere spring months in 2005 (Taylor et al., 2009) and in 2002 (Paulino et al., 2011, 2012). Fast gravity waves are less susceptible to dissipative filtering by molecular viscosity, which is the main filtering mechanism in the thermosphere. In the thermosphere, kinematic viscosity and thermal diffusivity damp gravity waves individually, depending on their intrinsic frequency, vertical wavelength, and intrinsic phase speed (e.g., Vadas and Fritts, 2005; Vadas, 2007). However, the spatial characteristics of the gravity waves (wavelength) should be taken into account. When a gravity wave propagates into the thermosphere, the kinematic viscosity and thermal diffusivity act in order to produce damping for the wave (e.g., Vadas and Fritts, 2005; Vadas, 2007).

Vadas (2007) ray-traced many gravity waves from the troposphere and lower thermosphere into the thermosphere, and

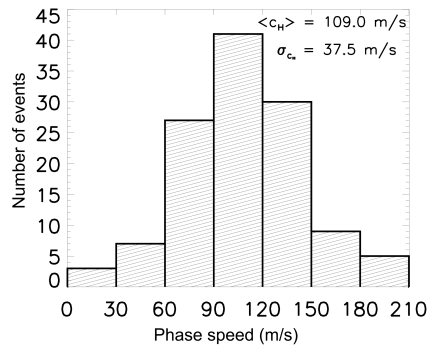


Figure 4. Histogram for the observed horizontal phase speed.

determined their propagation characteristics and dissipation altitudes. She found that horizontal wavelengths longer than 100 km are necessary in order for gravity waves to reach $z \geq 200$ km (Fig. 9b from Vadas, 2007). This is consistent with our results here (shown in Fig. 4). Additionally, that work shows that the vertical wavelengths must be at least 40 km. This is also consistent with our results, because a long vertical wavelength is necessary in order for a gravity wave to be observed in the OI6300 airglow emission. In particular, a gravity wave must have $\lambda_z \gg 40$ km in order to be observed in the OI6300 emission layer, since the OI6300 emission layer thickness is ~ 80 km (Sobral et al., 1993).

In general, a gravity wave reaching $z > 200$ km must have an intrinsic phase speed of at least 100 m s^{-1} (Vadas, 2007). Since the wind is unknown, the intrinsic phase speeds could not be calculated. However, our range of observed phase speeds as shown in Fig. 4 is consistent with this result. Neither medium-scale nor small-scale (bands and ripples) gravity waves observed in the MLT region by airglow images in previous works have the same necessary period and wavelength patterns simultaneously. This suggests that the sources of the gravity waves observed in the OI6300 images are likely different from the sources of the MLT gravity waves. For example, these gravity waves may have their sources associated with thermospheric body forcing or heating in the lower thermosphere (Vadas and Liu, 2009; Vadas and Crowley, 2010; Vadas, 2013). Some of these waves may even be generated by the Perkins mechanism.

3.2 Propagation direction

Figure 5 shows the propagation direction of all of the 98 periodic waves. A clear anisotropy of the propagation direction can be noticed. It seems that there are two preferential propagation directions: north and southeast. Most of the gravity waves propagated to the northeast, north or northwest. Another group of waves propagated to the southeast. Periodic waves propagating southwestward, westward and eastward were rare.

If most of these waves are assumed to be gravity waves (due to their spectral characteristics discussed in the

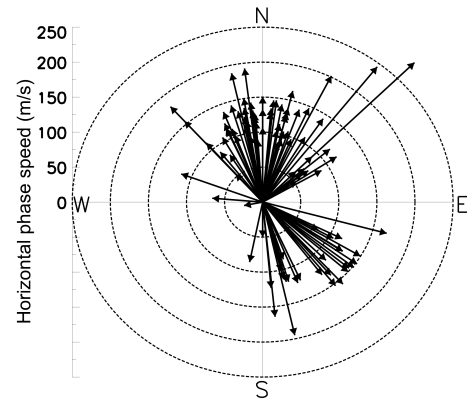


Figure 5. Horizontal phase speed diagram for all observed gravity waves. Arrows point in the direction of propagation of the gravity waves. The dashed lines indicate isolines of the same phase speed.

Sect. 3.1), there are two main factors which could create this observed anisotropy. The first factor is that gravity waves are filtered by the winds in the lower to mid-thermosphere (Fritts and Vadas, 2008). Combined with dissipative filtering, this process mainly preserves those gravity waves propagating opposite to the neutral wind. Those gravity waves propagating in the same direction as the wind have smaller λ_z , which causes the effects of molecular viscosity to be enhanced, thereby causing the waves to dissipate (Vadas, 2007). The second factor is that the source of the gravity waves may be anisotropic (either for each individual source or for the location of the sources relative to the observation location).

Fukushima et al. (2012) reported a long period study on wave structures observed in OI6300 airglow images over Indonesia. They found that the dominant propagation direction is to the south, which does not agree with the present observations. They also suggested that the origin of these waves was due to the penetration of gravity waves in the thermosphere.

MSTIDs generated by the Perkins instability can be observed at mid- and low latitudes during nighttime. They usually propagate in the Perkins phase front normal direction (Perkins, 1973). A portion of the waves observed in this work had this characteristic. According to Kelley (2011), even MSTIDs generated at high latitudes can reach the tropics if they propagate along this direction. Observations have confirmed this (e.g., Kubota et al., 2000).

For our data set here, it is not likely that the Perkins instability or the sporadic E layer instability was the main mechanism for generating the observed waves, because most of them are not heading in the Perkins phase front normal direction. There are few waves propagating eastward and westward, which could easily be explained by gravity wave source, wind and dissipative filtering processes. There is a set of waves that has Perkins' phase front direction, i.e., the waves which propagated to the southeast; however, the observations close to the Equator exclude the possibilities of these

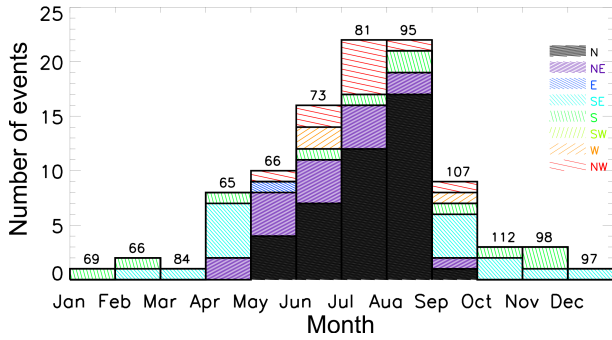


Figure 6. Annual distribution of the gravity waves. The number of the observed cloudless nights are shown at the top of the bars.

waves being generated by the Perkins process. On the other hand, the few waves propagating to the northwest could have their origin in the Perkins instability at midlatitudes, but this cannot be confirmed by using only airglow images.

The propagation direction of gravity waves observed in the mesopause region, at the same site of observation (Medeiros et al., 2007; Taylor et al., 2009), revealed a distinct behavior, primarily, the large gravity waves, which have a well-defined propagation direction to the east and northeast. This was another reason to believe that the present waves must have their origin in the lower thermosphere.

3.3 Seasonality and solar activity

The present data have a long period of observation, such that the seasonality and solar cycle dependence on the wave activity could be studied. Figure 6 shows the occurrence of the waves and their respective propagation direction as a function of the months. Most of the periodic waves were observed from April to October. Waves with azimuth between 337.5° and 22.5° were considered to be propagating northward, waves with azimuth between 22.5° and 67.5° were considered propagating northeastward, etc. For example, periodic waves propagating northward and northeastward only appeared during the winter months. Waves propagating southward were observed in almost all months, but only for a few events. Even though the number of observed cloudless nights (as shown at the top of the bars in Fig. 6) was reduced in the first half of the year, this can not be the reason for the present seasonality because there were more nights of observation in September, October, November and December, and few waves were observed as well.

A simple analysis of the thermospheric wind pattern is useful for understanding those results. Gravity waves propagating in the same direction as the wind may easily reach critical levels and be absorbed by the background atmosphere (e.g., Vadas, 2007). According to Meriwether et al. (2011), the meridional wind in Brazilian equatorial region, derived from a Fabry–Pérot interferometer located at the Cajazeiras Observatory (38.56° W, 6.89° S), blows toward the south dur-

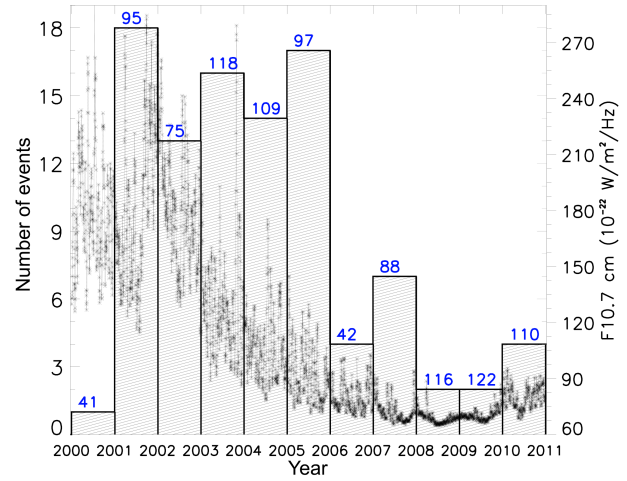


Figure 7. Occurrence of the gravity waves from 2000 to 2011, together with the solar flux 10.7 cm. The number of the observed cloudless nights are shown at the top of the bars.

ing the Southern Hemisphere winter months (June, July, and August), primarily at the beginning of the night. This is the period of the higher occurrence of the periodic waves, and most of them are propagating against the background wind; i.e., they propagated to the north. Moreover, none of the waves propagating northward were observed during the summer months (December, January, and February), when the wind was predominately blowing to the north.

In order to investigate the possible effect of solar activity on the occurrence of these waves in the thermosphere, the solar flux F10.7 cm is plotted together with the monthly occurrence of the wave events in Fig. 7. Again, the data cover almost an entire solar cycle. It seems that the occurrence of periodic waves depends on the solar activity. However, this occurrence rate does not strictly follow the solar cycle in the years 2000, 2005 and 2007. It is important to observe that in 2000, 2002 and 2006 there were 41, 75 and 42 nights observed, respectively; i.e., there were few observed nights compared to the closer years. Periodic waves observed in the OI6300 for the Northern Hemisphere were more common during the winter as well (Garcia et al., 2000). Small-scale gravity waves, observed in the MLT at São João do Cariri (Medeiros et al., 2004), were also observed more frequently during the winter.

3.4 Influence of the magnetic activity

The magnetic activity during the time of observation is shown in Fig. 8, and most of the observed periodic waves had durations shorter than 1.5 h (not shown here). These periodic waves were mostly observed during quiet geomagnetic conditions, and the number of wave events was fairly independent of Kp for Kp = 0 to 5. This suggests that these events occurred predominately during the low magnetic activity. Thus,

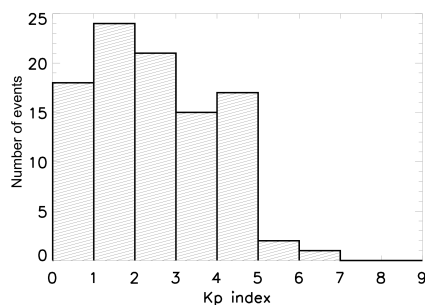


Figure 8. Distribution of the gravity waves according to the geomagnetic activity as indicated by the Kp index during the time of observation of the gravity waves.

geomagnetic activity does not appear to be an important factor for observing these wave structures in the OI6300 airglow images.

4 Summary and conclusions

Observations carried out at São João do Cariri from September 2000 to November 2010 revealed characteristics of 98 periodic waves observed in the OI6300 airglow images. These waves had horizontal wavelengths which ranged from 100 to 200 km and periods which ranged from 5 to 45 min. Most of the periodic waves propagated to the northwest and northeast. The other group of waves propagated mainly southeastward and southward.

Typical phase speeds were between 60 and 150 m s⁻¹, with a few up to 210 m s⁻¹. Most of the waves were observed during the magnetically quiet nights. It was found that the periodic wave occurrence rate follows the solar activity. A clear seasonal dependence of these events, with a predominant occurrence during the winter months, was also observed. The present waves were quasi-periodic, and most of them looked completely different than the MSTIDs observed in Brazil and reported previously. Based on their characteristics, most of these waves was identified as gravity waves rather than Perkins' waves. Note also that most of the waves did not propagate perpendicular to the Perkins phase front direction. The present results were compared to the gravity wave theory, and good agreement, in terms of horizontal wavelengths and phase speeds, was found as well.

The Supplement related to this article is available online at doi:10.5194/angeo-34-293-2016-supplement.

Acknowledgements. I. Paulino thanks the Conselho Nacional de Desenvolvimento Científico e Tecnológico (CNPq) for the support of this research under grants no. 453565/2013-1 and

no. 478117/2013-2. Part of this research was also supported by the Fundação de Amparo à Pesquisa do Estado de São Paulo (FAPESP), grant no. 2011/20120-5. S. L. Vadas was supported by NASA contract NNH12CE58C.

The data used to produce the results of this manuscript were obtained from the Observatório de Luminescência Atmosférica da Paraíba at São João do Cariri, which is supported by the Universidade Federal de Campina Grande and Instituto Nacional de Pesquisas Espaciais. If someone would like to access these data, please contact either Amauri F. Medeiros (afragoso@df.ufcg.edu.br) or Hisao Takahashi (hisao.takahashi@inpe.br).

The topical editor, A. J. Kavanagh, thanks the two anonymous referees for help in evaluating this paper.

References

- Afraimovich, E. L., Kosogorov, E. A., Leonovich, L. A., Palamartchouk, K. S., Perevalova, N. P., and Pirog, O. M.: Determining parameters of large-scale traveling ionospheric disturbances of auroral origin using GPS-arrays, *J. Atmos. Sol.-Terr. Phys.*, 62, 553–565, doi:10.1016/S1364-6826(00)00011-0, 2000.
- Amorim, D. C. M., Pimenta, A. A., Bittencourt, J. A., and Fagundes, P. R.: Long-term study of medium-scale traveling ionospheric disturbances using O I 630 nm all-sky imaging and ionosonde over Brazilian low latitudes, *J. Geophys. Res.-Space*, 116, A06312, doi:10.1029/2010JA016090, 2011.
- Candido, C. M. N., Pimenta, A. A., Bittencourt, J. A., and Becker-Guedes, F.: Statistical analysis of the occurrence of medium-scale traveling ionospheric disturbances over Brazilian low latitudes using OI 630.0 nm emission all-sky images, *Geophys. Res. Lett.*, 35, L17105, doi:10.1029/2008GL035043, 2008.
- Clemesha, B. and Batista, P.: Gravity waves and wind-shear in the MLT at 23° S, *Adv. Space Res.*, 41, 1472–1477, doi:10.1016/j.asr.2007.03.085, 2008.
- Deng, Z., Schön, S., Zhang, H., Bender, M., and Wickert, J.: Medium-scale traveling ionospheric disturbances (MSTID) modeling using a dense German GPS network, *Adv. Space Res.*, 51, 1001–1007, doi:10.1016/j.asr.2012.07.022, 2013.
- Francis, S. H.: A theory of medium-scale traveling ionospheric disturbances, *J. Geophys. Res.*, 79, 5245–5260, doi:10.1029/JA079i034p05245, 1974.
- Frissell, N. A., Baker, J. B. H., Ruohoniemi, J. M., Gerrard, A. J., Miller, E. S., Marini, J. P., West, M. L., and Bristow, W. A.: Climatology of medium-scale traveling ionospheric disturbances observed by the midlatitude Blackstone SuperDARN radar, *J. Geophys. Res.-Space*, 119, 7679–7697, doi:10.1002/2014JA019870, 2014.
- Fritts, D. C. and Alexander, M. J.: Gravity wave dynamics and effects in the middle atmosphere, *Rev. Geophys.*, 41, 1003, doi:10.1029/2001RG000106, 2003.
- Fritts, D. C. and Vadas, S. L.: Gravity wave penetration into the thermosphere: sensitivity to solar cycle variations and mean winds, *Ann. Geophys.*, 26, 3841–3861, doi:10.5194/angeo-26-3841-2008, 2008.
- Fukushima, D., Shiokawa, K., Otsuka, Y., and Ogawa, T.: Observation of equatorial nighttime medium-scale traveling ionospheric

- disturbances in 630-nm airglow images over 7 years, *J. Geophys. Res.-Space*, 117, A10324, doi:10.1029/2012JA017758, 2012.
- Garcia, F. J., Kelley, M. C., Makela, J. J., and Huang, C.-S.: Airglow observations of mesoscale low-velocity traveling ionospheric disturbances at midlatitudes, *J. Geophys. Res.*, 105, 18407, doi:10.1029/1999JA000305, 2000.
- He, L.-S. and Ping, J.-S.: Occurrence of medium-scale travelling ionospheric disturbances identified in the Tasman international geospace environment radar observations, *Adv. Space Res.*, 42, 1276–1280, doi:10.1016/j.asr.2007.06.010, 2008.
- Hocke, K. and Schlegel, K.: A review of atmospheric gravity waves and travelling ionospheric disturbances: 1982–1995, *Ann. Geophys.*, 14, 917–940, doi:10.1007/s00585-996-0917-6, 1996.
- Ishida, T., Hosokawa, K., Shibata, T., Suzuki, S., Nishitani, N., and Ogawa, T.: SuperDARN observations of daytime MSTIDs in the auroral and mid-latitudes: Possibility of long-distance propagation, *Geophys. Res. Lett.*, 35, L13102, doi:10.1029/2008GL034623, 2008.
- Katamzi, Z. T., Smith, N. D., Mitchell, C. N., Spalla, P., and Materassi, M.: Statistical analysis of travelling ionospheric disturbances using TEC observations from geostationary satellites, *J. Atmos. Sol.-Terr. Phys.*, 74, 64–80, doi:10.1016/j.jastp.2011.10.006, 2012.
- Kelley, M. C.: On the origin of mesoscale TIDs at midlatitudes, *Ann. Geophys.*, 29, 361–366, doi:10.5194/angeo-29-361-2011, 2011.
- Kotake, N., Otsuka, Y., Tsugawa, T., Ogawa, T., and Saito, A.: Climatological study of GPS total electron content variations caused by medium-scale traveling ionospheric disturbances, *J. Geophys. Res.-Space*, 111, A04306, doi:10.1029/2005JA011418, 2006.
- Kubota, M., Shiokawa, K., Ejiri, M. K., Otsuka, Y., Ogawa, T., Sakanoi, T., Fukunishi, H., Yamamoto, M., Fukao, S., and Saito, A.: Traveling ionospheric disturbances observed in the OI 630-nm nightglow images over Japan by using a Multipoint Imager Network during the FRONT Campaign, *Geophys. Res. Lett.*, 27, 4037–4040, doi:10.1029/2000GL011858, 2000.
- Kutiev, I., Marinov, P., Fidanova, S., and Warnant, R.: Modeling medium-scale TEC structures, observed by Belgian GPS receivers network, *Adv. Space Res.*, 43, 1732–1739, doi:10.1016/j.asr.2008.07.021, 2009.
- MacDougall, J. W. and Jayachandran, P. T.: Solar terminator and auroral sources for traveling ionospheric disturbances in the midlatitude F region, *J. Atmos. Sol.-Terr. Phys.*, 73, 2437–2443, doi:10.1016/j.jastp.2011.10.009, 2011.
- Makela, J. J., Lognonné, P., Hébert, H., Gehrels, T., Rolland, L., Allgeyer, S., Kherani, A., Occhipinti, G., Astafyeva, E., Coisson, P., Loevenbruck, A., Clévéde, E., Kelley, M. C., and Lamouroux, J.: Imaging and modeling the ionospheric airglow response over Hawaii to the tsunami generated by the Tohoku earthquake of 11 March 2011, *Geophys. Res. Lett.*, 38, L00G02, doi:10.1029/2011GL047860, 2011.
- Martinis, C., Baumgardner, J., Wroten, J., and Mendillo, M.: All-sky imaging observations of conjugate medium-scale traveling ionospheric disturbances in the American sector, *J. Geophys. Res.-Space*, 116, A05326, doi:10.1029/2010JA016264, 2011.
- Medeiros, A., Buriti, R., Machado, E., Takahashi, H., Batista, P., Gobbi, D., and Taylor, M.: Comparison of gravity wave activity observed by airglow imaging at two different latitudes in Brazil, *J. Atmos. Sol.-Terr. Phys.*, 66, 647–654, doi:10.1016/j.jastp.2004.01.016, 2004.
- Medeiros, A. F., Taylor, M. J., Takahashi, H., Batista, P. P., and Gobbi, D.: An investigation of gravity wave activity in the low-latitude upper mesosphere: Propagation direction and wind filtering, *J. Geophys. Res.-Atmos.*, 108, 4411, doi:10.1029/2002JD002593, 2003.
- Medeiros, A. F., Fechine, J., Buriti, R. A., Takahashi, H., Wrasse, C. M., and Gobbi, D.: Response of OH, O₂ and OI5577 airglow emissions to the mesospheric bore in the equatorial region of Brazil, *Adv. Space Res.*, 35, 1971–1975, doi:10.1016/j.asr.2005.03.075, 2005.
- Medeiros, A. F., Takahashi, H., Buriti, R. A., Fechine, J., Wrasse, C. M., and Gobbi, D.: MLT gravity wave climatology in the South America equatorial region observed by airglow imager, *Ann. Geophys.*, 25, 399–406, doi:10.5194/angeo-25-399-2007, 2007.
- Mendillo, M., Baumgardner, J., Nottingham, D., Aarons, J., Reinisch, B., Scali, J., and Kelley, M.: Investigations of thermospheric-ionospheric dynamics with 6300-Å images from the Arecibo Observatory, *J. Geophys. Res.*, 102, 7331–7344, doi:10.1029/96JA02786, 1997.
- Meriwether, J. W., Makela, J. J., Huang, Y., Fisher, D. J., Buriti, R. A., Medeiros, A. F., and Takahashi, H.: Climatology of the nighttime equatorial thermospheric winds and temperatures over Brazil near solar minimum, *J. Geophys. Res.*, 116, A04322, 0148–0227, 2011.
- Narayanan, L. V., Shiokawa, K., Otsuka, Y., and Saito, S.: Airglow observations of nighttime medium-scale traveling ionospheric disturbances from Yonaguni: Statistical characteristics and low-latitude limit, *J. Geophys. Res.-Space*, 119, 9268–9282, doi:10.1002/2014JA020368, 2014.
- Nicolls, M. J., Vadas, S. L., Aponte, N., and Sulzer, M. P.: Horizontal parameters of daytime thermospheric gravity waves and E region neutral winds over Puerto Rico, *J. Geophys. Res.-Space*, 119, 575–600, doi:10.1002/2013JA018988, 2014.
- Otsuka, Y., Shiokawa, K., Ogawa, T., and Wilkinson, P.: Geomagnetic conjugate observations of medium-scale traveling ionospheric disturbances at midlatitude using all-sky airglow imagers, *Geophys. Res. Lett.*, 31, L15803, doi:10.1029/2004GL020262, 2004.
- Otsuka, Y., Onoma, F., Shiokawa, K., Ogawa, T., Yamamoto, M., and Fukao, S.: Simultaneous observations of nighttime medium-scale traveling ionospheric disturbances and E region field-aligned irregularities at midlatitude, *J. Geophys. Res.-Space*, 112, A06317, doi:10.1029/2005JA011548, 2007.
- Otsuka, Y., Tani, T., Tsugawa, T., Ogawa, T., and Saito, A.: Statistical study of relationship between medium-scale traveling ionospheric disturbance and sporadic E layer activities in summer night over Japan, *J. Atmos. Sol.-Terr. Phys.*, 70, 2196–2202, doi:10.1016/j.jastp.2008.07.008, 2008.
- Park, J., Lühr, H., Min, K. W., and Lee, J.-J.: Plasma density undulations in the nighttime mid-latitude F-region as observed by CHAMP, KOMPSAT-1, and DMSP F15, *J. Atmos. Sol.-Terr. Phys.*, 72, 183–192, doi:10.1016/j.jastp.2009.11.007, 2010.
- Paulino, I., Takahashi, H., Medeiros, A., Wrasse, C., Buriti, R., Sobral, J., and Gobbi, D.: Mesospheric gravity waves and ionospheric plasma bubbles observed during the

- COPEX campaign, *J. Atmos. Sol.-Terr. Phys.*, 73, 1575–1580, doi:10.1016/j.jastp.2010.12.004, 2011.
- Paulino, I., Takahashi, H., Vadas, S., Wrasse, C., Sobral, J., Medeiros, A., Buriti, R., and Gobbi, D.: Forward ray-tracing for medium-scale gravity waves observed during the COPEX campaign, *J. Atmos. Sol.-Terr. Phys.*, 90–91, 117–123, doi:10.1016/j.jastp.2012.08.006, 2012.
- Perkins, F.: Spread F and ionospheric currents, *J. Geophys. Res.*, 78, 218–226, doi:10.1029/JA078i001p00218, 1973.
- Pimenta, A. A., Amorim, D. C. M., and Candido, C. M. N.: Thermospheric dark band structures at low latitudes in the Southern Hemisphere under different solar activity conditions: A study using OI 630 nm emission all-sky images, *Geophys. Res. Lett.*, 35, L16103, doi:10.1029/2008GL034904, 2008.
- Saito, A., Fukao, S., and Miyazaki, S.: High resolution mapping of TEC perturbations with the GSI GPS Network over Japan, *Geophys. Res. Lett.*, 25, 3079–3082, doi:10.1029/98GL52361, 1998.
- Shiokawa, K., Ihara, C., Otsuka, Y., and Ogawa, T.: Statistical study of nighttime medium-scale traveling ionospheric disturbances using midlatitude airglow images, *J. Geophys. Res.-Space*, 108, 1052, doi:10.1029/2002JA009491, 2003.
- Shiokawa, K., Otsuka, Y., Tsugawa, T., Ogawa, T., Saito, A., Ohshima, K., Kubota, M., Maruyama, T., Nakamura, T., Yamamoto, M., and Wilkinson, P.: Geomagnetic conjugate observation of nighttime medium-scale and large-scale traveling ionospheric disturbances: FRONT3 campaign, *J. Geophys. Res.-Space*, 110, A05303, doi:10.1029/2004JA010845, 2005.
- Shiokawa, K., Otsuka, Y., and Ogawa, T.: Quasiperiodic southward moving waves in 630-nm airglow images in the equatorial thermosphere, *J. Geophys. Res.-Space*, 111, A06301, doi:10.1029/2005JA011406, 2006.
- Shiokawa, K., Mori, M., Otsuka, Y., Oyama, S., Nozawa, S., Suzuki, S., and Connors, M.: Observation of nighttime medium-scale travelling ionospheric disturbances by two 630-nm airglow imagers near the auroral zone, *J. Atmos. Sol.-Terr. Phys.*, 103, 184–194, doi:10.1016/j.jastp.2013.03.024, 2013.
- Smith, S. M., Vadas, S. L., Baggaley, W. J., Hernandez, G., and Baumgardner, J.: Gravity wave coupling between the mesosphere and thermosphere over New Zealand, *J. Geophys. Res.-Space*, 118, 2694–2707, doi:10.1002/jgra.50263, 2013.
- Sobral, J. H. A., Takahashi, H., Abdu, M. A., Muralikrishna, P., Sahai, Y., Zamlutti, C. J., de Paula, E. R., and Batista, P. P.: Determination of the quenching rate of the O(¹D) by O(³P) from rocket-borne optical (630 nm) and electron density data, *J. Geophys. Res.*, 98, 7791–7798, doi:10.1029/92JA01839, 1993.
- Sobral, J. H. A., Takahashi, H., Abdu, M. A., Taylor, M. J., Sawant, H., Santana, D. C., Gobbi, D., de Medeiros, A. F., Zamlutti, C. J., Schuch, N. J., and Borba, G. L.: Thermospheric F-region travelling disturbances detected at low latitude by an OI 630 nm digital imager system, *Adv. Space Res.*, 27, 1201–1206, doi:10.1016/S0273-1177(01)00198-3, 2001.
- Taylor, M. J., Bishop, M. B., and Taylor, V.: All-sky measurements of short period waves imaged in the OI(557.7 nm), Na(589.2 nm) and near infrared OH and O₂(0,1) nightglow emissions during the ALOHA-93 Campaign, *Geophys. Res. Lett.*, 22, 2833–2836, doi:10.1029/95GL02946, 1995.
- Taylor, M. J., Jahn, J.-M., Fukao, S., and Saito, A.: Possible evidence of gravity wave coupling into the mid-latitude F region ionosphere during the SEEK Campaign, *Geophys. Res. Lett.*, 25, 1801–1804, doi:10.1029/97GL03448, 1998.
- Taylor, M. J., Pautet, P.-D., Medeiros, A. F., Buriti, R., Fechine, J., Fritts, D. C., Vadas, S. L., Takahashi, H., and São Sabbas, F. T.: Characteristics of mesospheric gravity waves near the magnetic equator, Brazil, during the SpreadFEx campaign, *Ann. Geophys.*, 27, 461–472, doi:10.5194/angeo-27-461-2009, 2009.
- Vadas, S. L.: Horizontal and vertical propagation and dissipation of gravity waves in the thermosphere from lower atmospheric and thermospheric sources, *J. Geophys. Res.-Space*, 112, A06305, doi:10.1029/2006JA011845, 2007.
- Vadas, S. L.: Compressible f-plane solutions to body forces, heatings, and coolings, and application to the primary and secondary gravity waves generated by a deep convective plume, *J. Geophys. Res.-Space*, 118, 2377–2397, doi:10.1002/jgra.50163, 2013.
- Vadas, S. L. and Crowley, G.: Sources of the traveling ionospheric disturbances observed by the ionospheric TIDBIT sounder near Wallops Island on 30 October 2007, *J. Geophys. Res.-Space*, 115, A07324, doi:10.1029/2009JA015053, 2010.
- Vadas, S. L. and Fritts, D. C.: Thermospheric responses to gravity waves: Influences of increasing viscosity and thermal diffusivity, *J. Geophys. Res.-Atmos.*, 110, D15103, doi:10.1029/2004JD005574, 2005.
- Vadas, S. L. and Liu, H.: Generation of large-scale gravity waves and neutral winds in the thermosphere from the dissipation of convectively generated gravity waves, *J. Geophys. Res.-Space*, 114, A10310, doi:10.1029/2009JA014108, 2009.
- Vadas, S. L. and Nicolls, M. J.: Temporal evolution of neutral, thermospheric winds and plasma response using PFISR measurements of gravity waves, *J. Atmos. Sol.-Terr. Phys.*, 71, 744–770, doi:10.1016/j.jastp.2009.01.011, 2009.
- Vadas, S. L., Taylor, M. J., Pautet, P.-D., Stamus, P. A., Fritts, D. C., Liu, H.-L., São Sabbas, F. T., Rampinelli, V. T., Batista, P., and Takahashi, H.: Convection: the likely source of the medium-scale gravity waves observed in the OH airglow layer near Brasilia, Brazil, during the SpreadFEx campaign, *Ann. Geophys.*, 27, 231–259, doi:10.5194/angeo-27-231-2009, 2009.
- Waldock, J. A. and Jones, T. B.: Source regions of medium scale travelling ionospheric disturbances observed at mid-latitudes, *J. Atmos. Sol.-Terr. Phys.*, 49, 105–114, 1987.
- Yokoyama, T. and Hysell, D. L.: A new midlatitude ionosphere electrodynamic coupling model (MIECO): Latitudinal dependence and propagation of medium-scale traveling ionospheric disturbances, *Geophys. Res. Lett.*, 37, L08105, doi:10.1029/2010GL042598, 2010.
- Yokoyama, T., Otsuka, Y., Ogawa, T., Yamamoto, M., and Hysell, D. L.: First three-dimensional simulation of the Perkins instability in the nighttime midlatitude ionosphere, *Geophys. Res. Lett.*, 35, L03101, doi:10.1029/2007GL032496, 2008.
- Yokoyama, T., Hysell, D. L., Otsuka, Y., and Yamamoto, M.: Three-dimensional simulation of the coupled Perkins and E_s-layer instabilities in the nighttime midlatitude ionosphere, *J. Geophys. Res.-Space*, 114, A03308, doi:10.1029/2008JA013789, 2009.